



Structural Health Monitoring Of Composite Patch Repairs Using Embedded Fiber Bragg Grating Sensors and Neural Network Techniques

G.J. Tsamasphyros, N.K. Fournarakis, K. Kalkanis, A.C. Christopoulos,
G.N. Kanderakis.

The National Technical University of Athens,
Faculty of Applied Sciences, Dept. of Mechanics-Lab of Strength Materials, Zographou Campus,
Theocaridis Bld., GR-015773, Athens, Greece

Abstract- Modern developments in the space of aeronautics render explicit the need for exploitation of air structures up to their designed structural life or even further and consequently the need for adoption of maintenance techniques supporting their structural integrity in an acceptable, according to their designed criteria, manner. One of the most promising techniques is the so called "composite patch repair method", a method capable to repair cracked metallic structures using adhesively bonded composite patches, that constitutes an effective method for re-establishment of structural integrity. However, even though this method has important advantages, problems concerning the long-term behavior of the adhesive, the appearance of debonds, etc. appear and have led to the considerable delayed widespread acceptance of this method.

In the present study the realization and implementation of elements of a structural health monitoring system for composite patch repairs is being performed, combining elements from the theory of structural repair mechanics, the theory of intelligent materials and structures and particularly the technology of optical sensors and neural networks.

The study has been split in two parts: in the first part a presentation of the experimental set up as well as the subsequent experimental results are presented. Two major potential failures have been considered and studied experimentally: the repaired crack extension despite the repair and debond of the adhesive bonding of the composite onto the metallic structure.

In the second part, the inverse problem of fault detection, qualification / quantification and life expectancies are studied using neural network techniques. Various network learning algorithms are evaluated for the corresponding failure cases and comparison results are developed. The data taken from the experimental test series (part I of the study) are used as network exemplars for training/test reasons and the corresponding deviations are calculated as well as the network performance metrics.

Keywords: Composite Patch Repair, Bragg Grating Sensors, Neural Network Analysis, F.E. Analysis

1. Introduction

Current economic world conditions are forcing to the operation of both military and civilian aircraft well beyond their original design life, resulting in innovative repair techniques. The recent development of high strength fibres and adhesives has led to the invention of a new methodology for the repair of metallic structures by the adhesive bonding of patches manufactured by composite materials. Bonded repairs are mechanically efficient, cost effective and can be applied rapidly to produce an inspectable damage tolerant repair. Even though the technique presents great advantages from a life cycle cost point of view for the aeronautic structures, the certification of the method for operational usage is not yet completed. Problems such as the long term stability of the adhesive bonding, precludes the method from a widespread acceptance as a field repair technique.

In order to advance the potential spreading of the composite patch repair technique, on line health monitoring should be adapted to secure the long term stability and the structural integrity of the repair and the structure as a whole. In that respect and in order to enable on line monitoring of the local stress field into a composite patch during a potential failure, such as crack or debond propagation, optical fiber sensors can be structurally integrated into it. Fiber optic sensors became lately a main research area in the field of "Smart Structures" because of the significant advantages they offer compared to previous efforts in the area of stress-strain monitoring (e.g. strain gages, etc.). Various types of sensors can be intrinsically embedded in a composite material, like the Bragg Grating, Fabry-Perrot, the Polarimetric, etc. On the contrary, there are not many candidate fiber sensors in the case of a composite patch due to the miniature dimensions used, the single fiber embedding and interface requirement, the requirement to trace a single, decoupled strain component, etc. Therefore, in the present study, Fiber Bragg grating sensors were embedded in the composite patches, to trace the mechanical field variations. The field variations, for simplicity reasons, were

assumed mechanical only, decoupled from any thermal effect, by keeping the environmental conditions stable during the experimental study.

The modern systems expressing structural health monitoring (SHM) philosophy are split in two main categories [1]:

- Monitoring using load spectrum:
- Health monitoring systems:

Moreover, the level of integration of the system defines the model of sensing and damage logic required for a specific application. For example a system designed to monitor the health of a large scale structural element (a bridge) should use global approach techniques using distributed sensing elements, due to the fact that a point-wise system resolution is not required. On the other hand, for the case of monitoring a crack propagating on the skin of an aircraft, where high strain resolution is required, a local sensing technique should be preferred combined with the proper damage logic.

The damage logic itself is expressed by the two following techniques [2]:

- Logic based on analytical/numerical models that apply to the specific structure or a family of identical structures, having predetermined field distributions for each discriminated fault signature.
- Logic based on decoupled from the structure itself numerical techniques, that do not take into account the geometry or the constituents of the structure but are based on existing load experience and field mapping. Such techniques are based on statistical models, on neural networks, on genetic algorithms or any combination of these.

PART I

1. Specimen design

Various specimens were designed and manufactured. The behavior and the repeatability of the strain measurements taken from the Bragg sensors should be evaluated as well as the durability of the sensor during the test process. Three specimens (Type I) were manufactured, according to the geometrical characteristics presented in Figure 1.

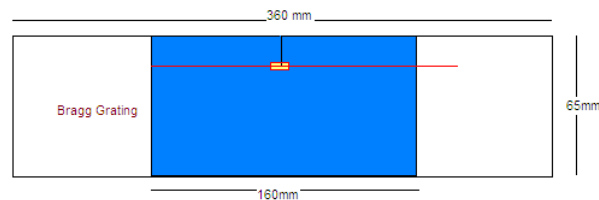


Figure 1: Measurement repeatability specimen (Type I).

The materials used, considered isotropic, are presented on Table 1.

Table 1: Material properties

Material	Thickness(m)	E (MPa)	G (MPa)	ν
Aluminium 2024-T3	6	72000	26900	0.3
Textron 5521 Prepreg	0.125 per lamina	207000	4800	0.21
FM73 Film Adhesive	0.2	---	750	---
Optical Fiber	Diameter 0,1mm	70000		0.29

The vertical projection of the crack tip was chosen as the sensor location, based on the numerical simulation results presented in [3-7]. The composite patch used was manufactured using six laminates of carbon epoxy prepreg. The sensor was embedded between the third and fourth lamina, based on the results of [6]. The physical characteristics of the sensors were the following:

- Center wavelength $\lambda_B = 1535 \pm 10$ nm
- $\Delta\lambda = \sim 0.7$ nm
- Reflectivity $R = 85 \sim 97$ %
- Sensor length $L = 2$ mm

The specimens were subjected to tensile loading using an Instron test machine. The specimens were gradually loaded to a range of 1 to 10 KN tensile load and measurements for each load condition were recorded from the optical fiber sensors. A COTS Micron Optics Bragg Interrogator had been used for the acquisition of measurements, having the capability to store digitally the wavelength shifts of the sensors during the loading process.

Moreover, specimens were manufactured in order to study potential fault propagation. Taking into account that the faults studied were the crack or debond propagation, the specimens of Figure 2 were manufactured (Type II). Each of these specimens represented a potential debond (yellow area) developed in the area of the crack tip, between the composite patch and the repaired metallic area. The aim of the test series was to examine the possible propagation patterns of the cracked and/or debond area, using NDI techniques. Fiber optic sensors were not embedded in these specimens, due to the fact that measurements should not be taken. The specimens, manufactured using the materials of table 2 with a6-ply composite patch, were submitted to fatigue testing, using the following load data:

- Mean load : 2,1 tn
- Amplitude : 1,9 tn
- Load frequency : 10 Hz

Finally, in order to monitor the propagation of a failure in a composite patch repair, more specimens were manufactured, having embedded optical fiber sensors, as presented in Figure 3. Each of these specimens had two embedded optical sensors, in positions determined after the experimental study of specimens type II, using the same materials and sensors of specimens type I and II. The crack tip sensor was called as sensor “a” while the second sensor was called “b”. The loading conditions of the specimens were identical with the conditions of type II specimens.

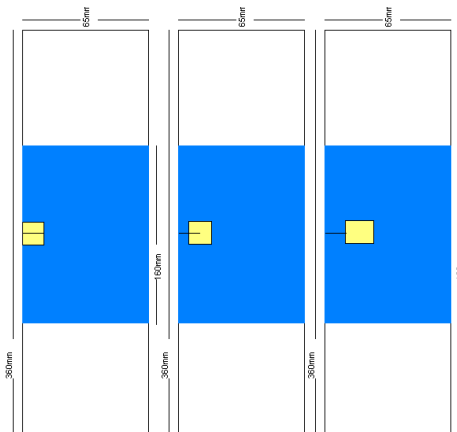


Figure 2: Fault propagation study specimens (type II-1, 2 and 3 respectively).

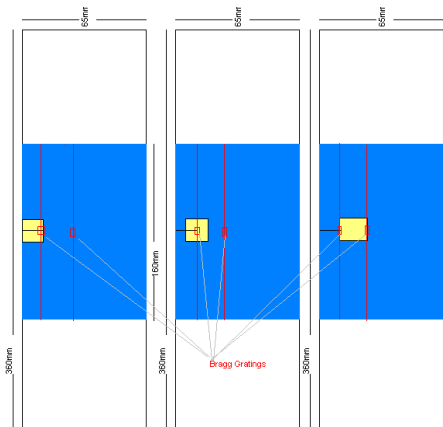


Figure 3: Monitored specimens (type III-1, 2 and 3 respectively).

For each of the above, three specimens were manufactured in order to secure the experimental results. The exact specimen details are presented in Table 2.

Table 2: Specimen type III details

Specimen Code	III-1			III-2			III-3		
	A	D	G	B	E	H	C	F	I
FBG a – Center Wavelength (nm)	1551,24	1551,28	1563,47	1551,12	1551,59	1562,36	1551,8	1551,34	1551,51
FBG b - Center Wavelength (nm)	1551,32	1551,26	1530,14	1551,65	1551,52	1551,82	1551,4	1551,89	1551,39
FBG a – Reflectivity (%)	99	98	97,8	98,6	98,8	97,1	99,3	98,9	97,6
FBG b - Reflectivity (%)	97,5	98,75	32,9	98,4	98,9	97,9	93	98,75	98,8



The data acquisition during the fatigue loading of type III specimens was based on the following technique:

- Measurement of crack length at 10K cycles and every 2.5K cycles with simultaneous sensor wavelength shift recording
- Measurement of debond area using C-Scan NDI every 10K cycles
- Ramp type tensile loading every 10K cycles with simultaneous sensor wavelength shift recording

1.1 Experimental Results – Specimen Type I & II

The results of the tensile loading of type I specimens are presented in Figure 4. It is shown that the repeatability of measurements is very satisfying and the strain measuring capability of the sensor is accurate, therefore the sensors were found to be appropriate for the experiment.

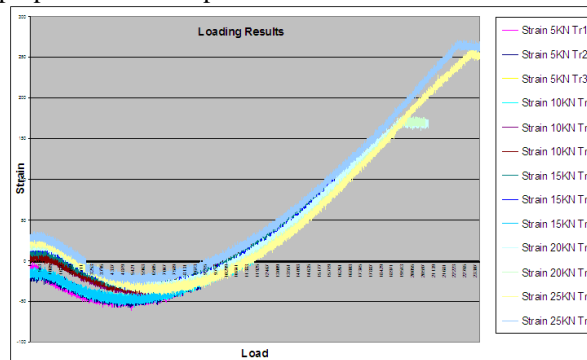


Figure 4: Load vs. Strain results during the repeatability test series

It was also found that during the initial tensile loading, compressive loads are developed near the crack tip, due to the fact that the specimen has a resulted curvature from the curing process because of the thermal coefficient mismatch of the patch and the aluminum material.

The results of the specimen type II loading, with respect to crack extension, are presented in Figure 5.

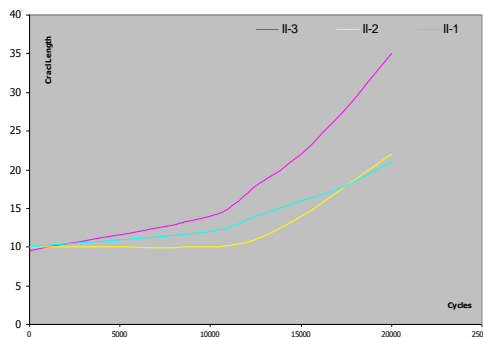


Figure 5: Crack extension of specimens type II

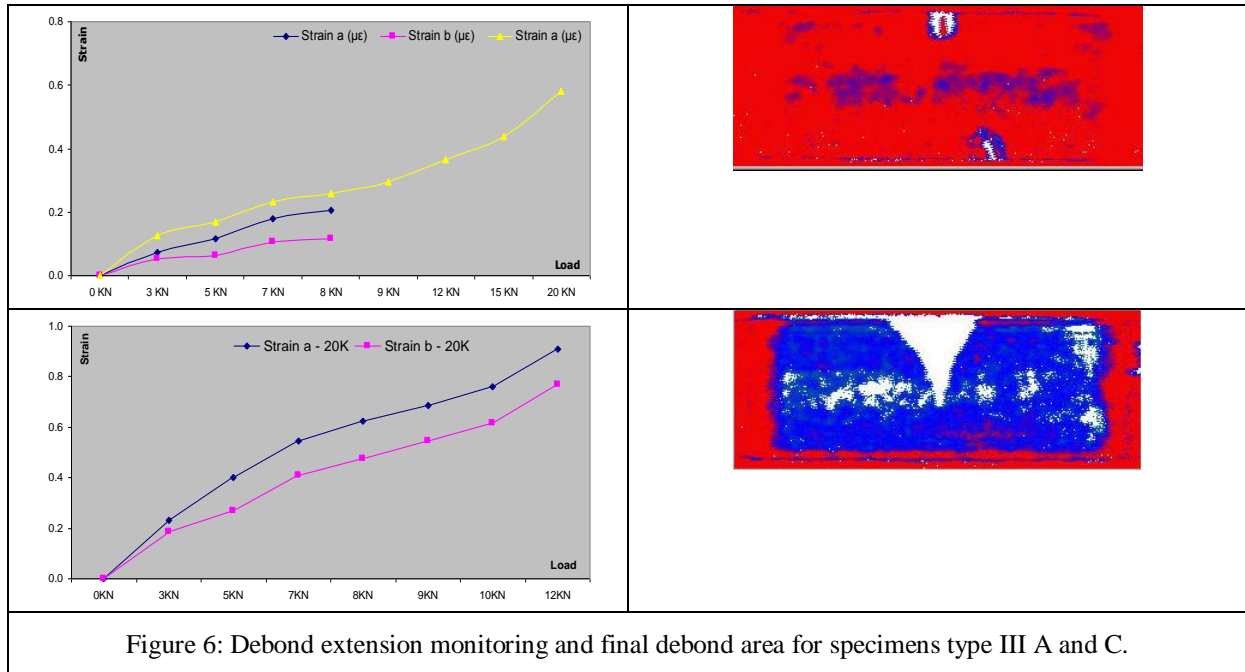
Moreover, C-Scan NDI was performed on these specimens in order to check the debond propagation due to the fatigue loading. From the results of the studies it was found that the crack propagated faster on the specimen type II-3 compared to the specimen type II-1 or 2. From these results it was obvious that specimens type II-3 were more prone to damage compared to the other two specimens. These results are self explanatory since the position of the debond of specimen type II-3 results in a more stress intensive crack tip area as compared to the other specimens, due to the fact that all loads are undertaken by the structure and not the patch at the specific area.

1.2 Experimental Results – Specimen Type III

Following the above described test procedure, various results were taken from the fiber optic sensors during the testing of specimens type III. The results are divided in two major categories: results related to the debond extension and results related to the crack propagation.

1.2.1 Debond Extension

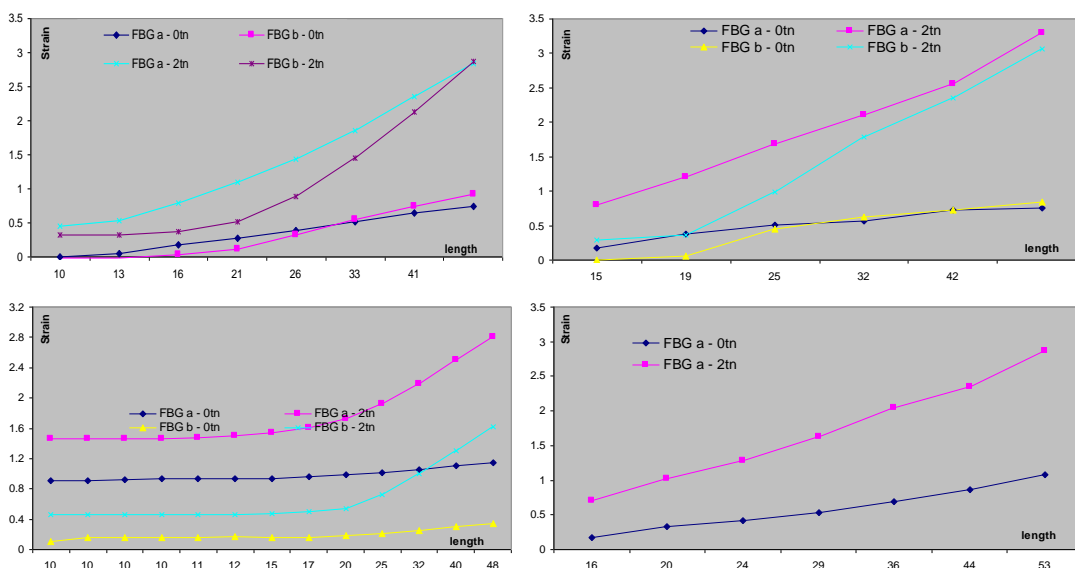
The measured results for a number of specimens of Table 2, in accordance with the bond extension monitoring, are presented in Figure 6.



From the above results it is obvious that, during the ramp loading, there is a shift in strain measurement due to the fact that the debond has propagated and resulted in a field alternation near the fiber optic sensors. The amount of debond extension determines the strain shift for the sensors.

1.3 Crack Propagation

The measured results for each specimen of Table 2, in accordance with the crack propagation monitoring, are presented in Figure 7.



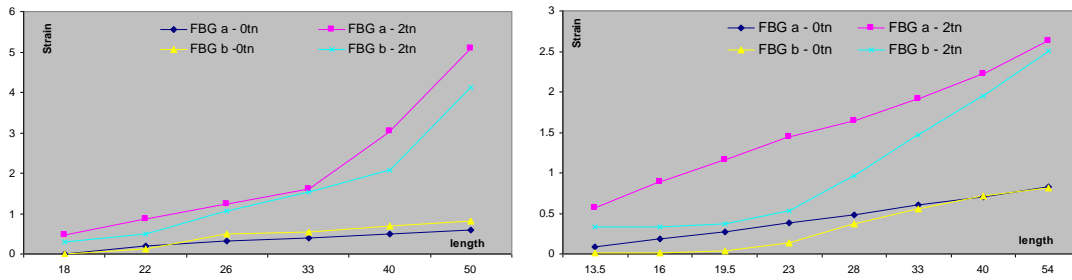


Figure 7: Crack Propagation monitoring for specimens type III B, C, D, E, F and G.

From the above results, a strain increment is obvious during the crack propagation. Moreover, for the sensor “b” of each specimen, a sudden strain increment was noticed when the crack was passing through the vertical level of the sensor.

1.4 Result Analysis

Taking into account the above results, a study was made to relate the measured results with the propagating failure. Considering the crack propagation as the major failure that could lead to the degradation of the repair strength and the final structure failure, the above data were further analyzed, assuming that:

- A: strain of sensor a
- B: strain of sensor b
- ΔA : strain increase of sensor a
- ΔB : strain increase of sensor b
- Δa : crack length increase

Using this notation, the test results for the crack propagation failure case, are presented in Figure 8.

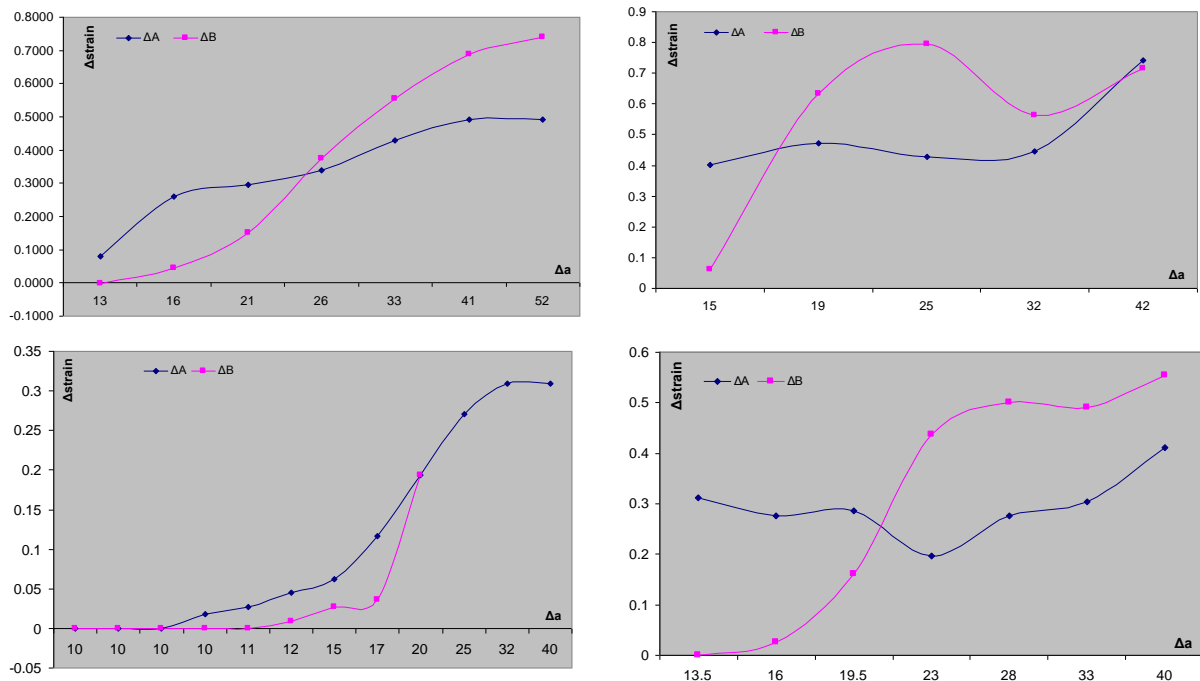


Figure 8: Strain increment due to crack propagation for specimens type III B, C, D and G.

From the above figure, it is obvious that during the crack propagation and when the crack “passes” from sensor “b”, the increment curves of the two sensors cross each other, giving a notion of the crack length on that time. Relevant curves can be developed for the case of the debond propagation, presenting the capability of the sensors to trace a failure propagation in the repaired structure.

PART II

According to the level of detail required by a health monitoring and damage identification system, four levels of logic implementation can be used [8]:

- Level 1: Damage verification and identification
- Level 2: Damage localization
- Level 3: Damage quantification
- Level 4: Life expectancy

In the present work, the use of neural networks and genetic algorithms was studied with specific application in a composite patch adhesively bonded to a crack metallic structure, in order to implement a structural integrity logic (four levels of implementation) concept in terms of health monitoring of the repair. In that respect, various learning algorithms are examined and compared using the data set defined above.

2. Neural Network Analysis

In order to design the best solutions available for each level of implementation, two main network types were used: a classification network and a function approximation network. Each network was used for a specific level of implementation. Thus, for levels 1 and 2 a classification network was used while for levels 3 and 4 a function approximation multilayer perceptron network was used. For further information on these types of networks, the reader is advised to refer to [9] and [10].

2.1 SHM LEVEL 1

For the implementation of the capability to identify and verify fault that occurred in a composite patch repair, due to the lack of experimental data, the learning data set used was produced using the finite element method, for the model presented on Figure 9.

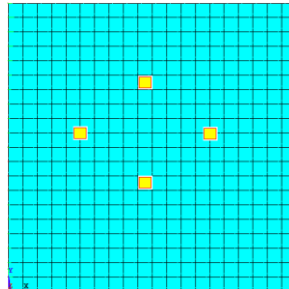


Figure 9: The structure FE model and the assumed sensor positions

Three types of failure were model as typical failures that can occur in a composite patch, which are:

- Crack
- Local disturbance
- Delamination

The data set consisted of 500 exemplars (data points). The network used for the algorithm evaluation consisted of 10 to 30 hidden processing elements and the test was performed with 1000 to 5000 epochs (iterations). Using the Figure 12 strain measurements as inputs, for the various load cases, for a typical classification multi layer perceptron network using the momentum learning algorithm, where the network codification used, had the format (SHM Level) – (Learning Algorithm) (PE's) - (Epochs), MSE stands for Mean Square Error, NMSE is Nominal Mean Square Error and r is the correlation coefficient [10]. From the results provided, the best test error was achieved for the 1-MOM25-3000 network and was 13.44%. This error could be misinterpreted as high enough, but for the case of a classification network is acceptable since the major concern is the number of misclassifications (how many misclassifications happened in the test sample) and not the variations of the probability of classification (which for the specific case the mean probability to belong to the specific class of failure was 85% that is an acceptable result).

2.2 SHM LEVEL 2

Using the same approach as for the case of SHM Level 1, a typical classification multilayer perceptron was used to locate the potential damage occurred within a composite patch. Due to the monitoring capabilities provided in part I, three classes of failures were assumed for the case of a composite patch, which are presented in Figure 10.

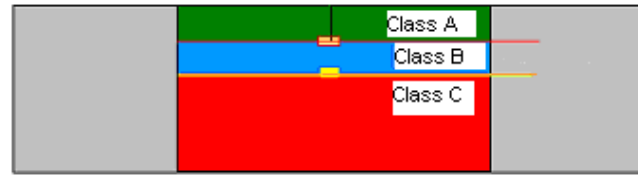


Figure 10: Classes of failure for SHM Level2

The data set was consisted of 850 exemplars (data points). The network used for the algorithm evaluation was consisted of 10 to 30 hidden processing elements and the test was performed with 1000 to 5000 epochs (iterations). Following the very same approach as in the case of SHM Level 1

From these results, it was found out that the minimum error was achieved using the 2-MOM30-1000 network and, generally, the error varied from 3.22% to 15.3%.

2.3 SHM LEVEL 3

Using the same approach with SHM Level 1& 2 networks, but instead using a function approximation network (Equation 1), for the mapping.

$$f(\varepsilon_z^{sensor1}, \varepsilon_z^{sensor2}) \rightarrow cracklength \quad \text{Equation 1}$$

It is obvious that the best network output is achieved using the 3-MOM25-2000 network architecture, while the error in all configurations varied between 2.19% and 8.3%.

2.4 SHM LEVEL 4

Finally, for the case of life expectancy of the repaired crack, having a propagating failure, using the same techniques as those in SHM Level 3 networks for the mapping (Equation 2).

$$f(\varepsilon_z^{sensor1}, \varepsilon_z^{sensor2}, N_{consumed}, cracklength) \rightarrow N_{expected} \quad \text{Equation 2}$$

It is obvious that the best network output is achieved using the 4-MOM20-3000 network architecture, while the error in all configurations varied between 3.53% and 17.32%.

2.5 Results

Having completed the training process as well as the validation of the network architectures for the given data set, the optimum network architecture for each SHM Level was submitted to a “live” process, during which real strain data (not training or validation set data) taken from the sensors were fed on the networks. The network outputs for this “unknown” data set were very good, close enough to the expected causes. For economy of space, the most interesting cases of network architectures for SHM Level 3 and 4 are presented in Figure 11.

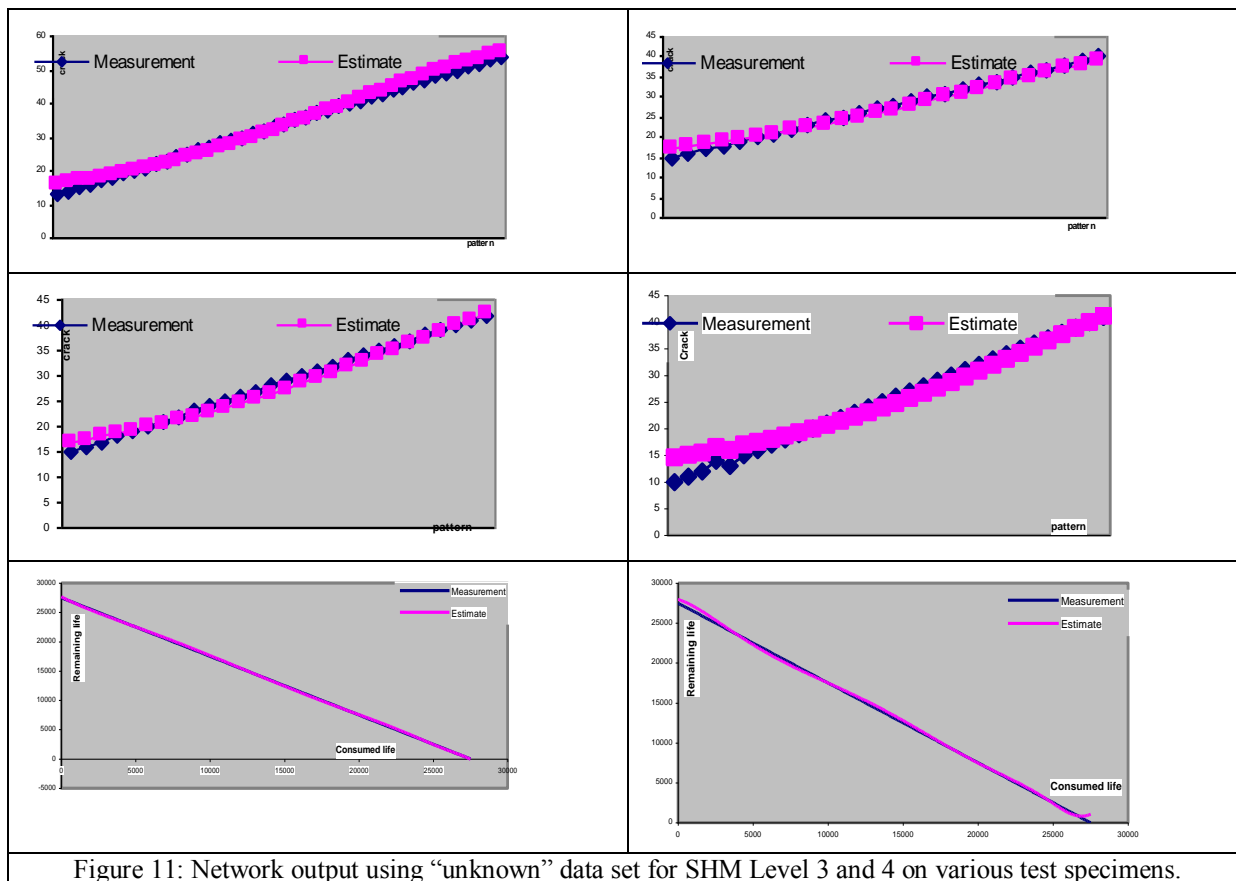


Figure 11: Network output using “unknown” data set for SHM Level 3 and 4 on various test specimens.

Similar results were achieved for the rest of the network architectures used for SHM Level 1, 2. Moreover, in order to check the stability of the solutions due to small data perturbations, uniform “noise” (from 1 to 5%) was added to the data input of the networks in order to evaluate their response. Due to the fact that a uniform type “noise” filter was added to the design of the networks, these small perturbations did not result to solution instability, but on the contrary, validated the stable performance of these networks as presented on Figure 12.

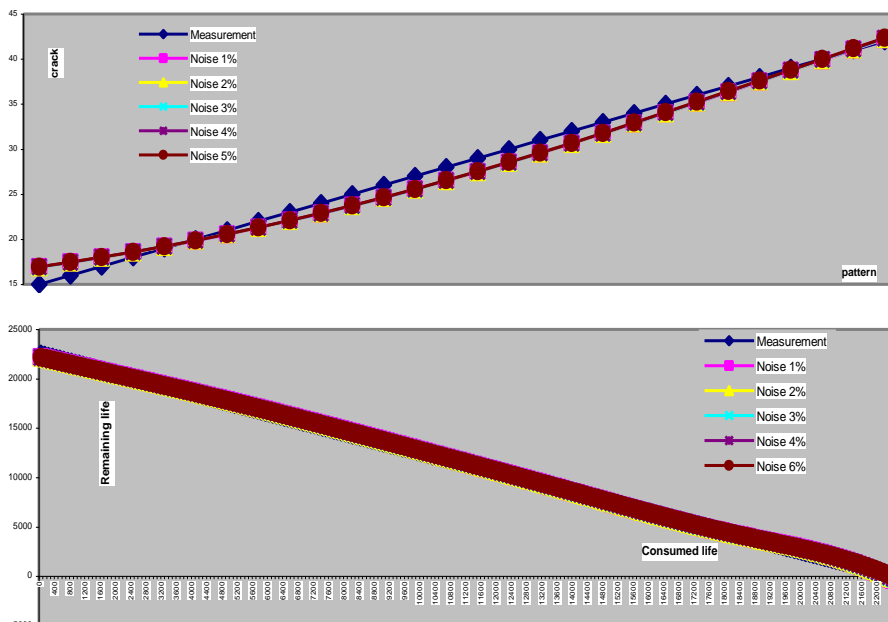


Figure 12: Network output stability testing SHM Level 3 and 4

3. Conclusions

Following the presented analysis, it was found out that, the inverse problem of fault detection, qualification / quantification and life expectancy of a composite patch repair, during its operational usage, can be treated using



neural network techniques and fiber optic sensors. The results achieved showed that the combination of fiber optic sensors and neural network damage prognosis and diagnosis capabilities can be considered to be a semi-integrated health monitoring system for the composite patch repair technique, ensuring the long term stability and durability of the repair.

4. ACKNOWLEDGEMENTS

The authors would like to thank the General Secretariat of Research and Development, Ministry of Education, Hellas as well as the Hellenic Aerospace Industry for the financial support and the facilities used during the present work.

5. References

- [1] W. Stawenski et al, Health Monitoring of Aerospace structures, Wiley, 2004.
- [2] W. Stawenski, MONITOR Research Program, EU IV Framework Program, 2001.
- [3] G. Tsamasphyros, G. N. Kanderakis, N.K. Furnarakis, Z. P. Marioli-Riga, Optimization of Embedded Optical Sensor Locations in Composite Repairs Applied Composite Materials Volume 10 No3: 129-140, May 2003, Kluwer Academic Publishers, Netherlands.
- [4] G.J. Tsamasphyros, N.K. Furnarakis, G.N. Kanderakis, Three Dimensional Finite Element Analysis of Composite Patches with Embedded Optical Fibres – Through Thickness Optimization, Z. P. Marioli-Riga “International Conference on Computational Engineering & Sciences, ICES’01, Puerto Vallarta, Mexico (2001).
- [5] G. J. Tsamasphyros, G. N. Kanderakis, N. K. Furnarakis, Z. P. Marioli-Riga, R. Chemama, R. Bartolo, Three – Dimensional Finite Element Analysis of composite patches with embedded optical fibers – Selection of Optical Fibers Paths and Sensors Locations, Structural Health Monitoring 2002, Daniel L. Balageas, 1203-1210, Destech Publications, ENS Cachan France, July 10-12, 2002.
- [6] G. J. Tsamasphyros, N. K. Furnarakis, G. N. Kanderakis, Z. P. Marioli-Riga, Three – Dimensional Finite Element Analysis of composite patches with embedded optical fibers – Optimizing Optical Fiber Embedding Location: Structural Health Monitoring 2002, Daniel L. Balageas, 1219-1226, Destech Publications, ENS Cachan France, July 10-12, 2002.
- [7] G. J. Tsamasphyros, G. N. Kanderakis, N. K. Furnarakis, Z. P. Marioli-Riga, Detection of patch debonding in composite repaired cracked metallic specimens, using optical fibers and sensors SPIE Optical Metrology Conference, 23-26 June 2003, Munich, Germany.
- [8] A. Rytter, Vibration Based Inspection of Civil Engineering Structures PhD Dissertation, Department of Building Technology and Structural Engineering, Aalborg University, Denmark, 1993
- [9] R. Rojas, Neural Networks: A Systematic Introduction, Springer, 1996
- [10] J. Principe, N. Euliano, Neural and Adaptive Systems: Fundamentals through Simulations, Wiley, 2000.